BULLETIN OF THE CHEMICAL SOCIETY OF JAPAN VOL. 43 2750—2758 (1970)

Fluorescence Quenching Reactions due to the Intermolecular Electron Transfer Process in Solution

Tadashi OKADA, Hiroo OOHARI and Noboru MATAGA*1

Department of Chemistry, Faculty of Engineering Science, Osaka University, Toyonaka

(Received April 13, 1970)

Mechanisms of the intermolecular electron transfer process in the electronically excited states of solute molecules have been studied in relation to the fluorescence quenching reactions in solution, employing pyrene as a fluorescer and some aromatic amine and cyano compounds as quenchers. The quenchers showed various strengths of the quenching actions which were classified and discussed on the basis of a new theoretical model of electron transfer process in excited state. Tetracyanoethylene showed a quite strong quenching action which was interpreted in terms of a long range electron transfer from excited pyrene to tetracyanoethylene. The relation between the exciplex formation, the electron transfer reaction due to the short range interaction and that due to the long range interaction have been discussed.

The mechanism of fluorescence quenching in solution has been studied for a long time.[1] Although there are diverse mechanisms of the luminescence quenching reactions, the intermolecular electron transfer or charge transfer processes in the excited state seem to be one of the most important mechanisms for fluorescence quenching reactions.[2] The mechanism may be connected with the fact that the electron affinity of a molecule is larger and its ionization potential is smaller in the electronically excited state than in the ground state and, the electron donor-acceptor interaction can arise in the excited state even though there is no interaction in the ground state. Recent studies[2] on exciplex (or heteroexcimer) luminescence are making important contributions to this fluorescence quenching mechanism.

The results of observations concerning exciplex fluorescence have indicated that the exciplex formed in a polar solvent by the encounter collision between the fluorescer (F*) and the quencher (L) molecule gradually shifts to the solvated ion-pair or to the dissociated ion-radicals during the lifetime of the excited state as follows:

$$F^* + L \underset{k_2}{\overset{k_1}{\rightleftarrows}} \text{exciplex} \xrightarrow{k_3} F_S^{\pm} \cdots L_S^{\mp} \rightarrow F_S^{\pm} + L_S^{\mp} \qquad (1)$$

Although Eq. (1) seems to be important for fluorescence quenching due to the electron transfer, it might not be correct to say that the electron transfer in the fluorescence quenching reaction occurs always *via* the formation of a "complex" where the interaction between the electron donor and the acceptor is considerable. In principle, it may be possible for the electron transfer to occur by very weak interaction in a quite loose encounter complex, so weak that the states of the system before and after the electron transfer can be regarded as independent stationary states between which the quantum mechanical transition occurs.[3] Accordingly, it is necessary and important to examine various quenchers of different strengths in detail for the elucidation of the electron transfer processes.

In the following, we show the results of our measurements on the quenching of pyrene fluorescence by various quenchers in various solvents.

Experimental

Materials. Pyrene was chromatographed on activated alumina and silica gel, and extensively

*1 To whom correspondence should be addressed.

1) Th. Förster, "Fluoreszenz Organisher Verbindungen," Vandenhoeck Ruprecht, Göttingen (1951).

2) H. Leonhardt and A. Weller, *Ber. Bunsenges. Phys. Chem.*, **67**, 791 (1963); N. Mataga, K. Ezumi and K. Takahashi, *Z. Phys. Chem. N.F.*, **44**, 250 (1965); N. Mataga, T. Okada and K. Ezumi, *Proc. International Conf. on Luminescence*, Budapest, 431 (1966); *Mol. Phys.*, **10**, 201, 203 (1966); T. Miwa and M. Koizumi, This Bulletin, **39**, 2603 (1966); N. Mataga, T. Okada and and N. Yamamoto, *ibid.*, **39**, 2562(1966); N. Mataga, T. Okada and H. Oohari, *ibid.*, **39**, 2563 (1966); N. Mataga and K. Ezumi, *ibid.*, **40**, 1355(1967); K. Kaneta and M. Koizumi, *ibid.*, **40**, 2254(1967); H. Knibbe, D. Rehm and A. Weller, *Z. Phys. Chem. N. F.*, **56**, 95, 99(1967); N. Mataga, T. Okada and N. Yamamoto, *Chem. Phys. Lett.*, **1**, 119 (1967); H. Beens, H.Knibbe and A. Weller, *J. Chem. Phys.*, **47**, 1183(1967); H. Knibbe, K. Rolleg, F. P. Schafer and A. Weller, *ibid.*, **47**, 1184 (1967); H. Knibbe, D. Rehm and A. Weller, *Ber. Bunsenges. Phys. Chem.*, **72**, 257 (1968); W. R. Ware and H. P. Richter, *J. Chem. Phys.*, **48**, 1595 (1968); T. Okada, H. Matsui, H. Oohari, H. Matsumoto and N. Mataga, *ibid.*, **49**, 4717 (1968).

3) N. Mataga and O. Tanimoto, *Theoret. Chim. Acta*, **15**, 111 (1969).

zone-refined. *N,N*-Dimethylaniline (DMA) was refluxed with acetic anhydride, washed with water, dried over potassium hydroxide, and distilled in a vacuum several times. G. R. grade tetracyanoethylene (TCNE) was recrystallized from monochlorobenzene and sublimated several times in a vacuum. 1,2,4,5-tetracyanobenzene (TCNB) was synthesized and purified in this laboratory.[4] Isomeric dicyanobenzenes (DCNB) were recrystallized from ethanol and sublimated in a vacuum. *n*-hexane was passed through a column of activated silica gel and distilled. Pyridine was refluxed with 28% aqueous solution of sodium hydroxide, dried over sodium hydroxide and potassium hydroxide and after refluxing with potassium hydroxide distilled carefully. Ethanol was treated with sulfuric acid and silver nitrate, dried over aluminium amalgam and activated silica gel, distilled carefully. Acetonitrile was refluxed repeatedly over phosphorus pentoxide, distilled into potassium carbonate and distilled from it. Spectrograde *N,N*-dimethylformamide (DMF) was used without further purification.

All solutions for the measurement were carefully deaerated by freeze-pump-thaw cycles.

Apparatus and Measurements. Fluorescence spectra were measured with an Aminco-Bowman spectrophotofluorometer which was calibrated to obtain the correct fluorescence quantum spectrum. Absorption spectra were measured by a Cary 15 spectrophotometer.

In order to measure the fluorescence decay times, the specimens were excited by a pulse which was made monochromatic through a monochromator (335 mμ). The fluorescence pulses were received by a photomultiplier of 1P28 type. Responses from the photomultiplier were guided to a synchroscope(Tektronix 585A) and the decay curve was photographed, or they were led to a sampling oscilloscope(Tektronix 661) and the decay curves were recorded on a X-Y recorder.

The exciting pulsed lights were produced by discharging a specially designed capacitor (of a few hundreds pF and charged up to 2000—4000 V) through a gap of about 0.5 mm between small platinum electrodes in air. The half width of the pulsed light was about 15 ns.

The measurement of the temperature effect on the fluorescence was conducted by using a metal dewar with quartz windows (for the temperature range below −50°C) or by using a quartz dewar which contains purified ethanol as a refrigerant (for measurements above −50°C). In the case of the former, the temperature of a solution in a quartz cuvette placed in the dewar was controlled by a constant flow of cold nitrogen gas. The flow of the gas was controlled by heating liquid nitrogen, and the temperature of the solution was measured by a thermocouple. In the case of the latter, the temperature of the solution in the cuvette was controlled by dropping appropriate amounts of liquid nitrogen into the refrigerant.

The measurements of the absorption spectra of transiently produced ion radicals were made by means of an ordinary flash photolysis apparatus. Both the first and the second flash lights have a half-value width of 3 μsec. The spectra were photographed by using a Shimazu GE 100 type spectrograph.

Experimental Results and Discussion

In such polar solvents as ethanol, DMF and acetonitrile, the fluorescence of pyrene is quenched by DMA completely. As an example, the quenching curves in acetonitrile and DMF are shown in Fig. 1, where the simple Stern-Volmer equation (2) is well satisfied with respect to the fluorescence quantum yield as well as the fluorescence decay time.

$$\eta'_F/\eta_F = \tau'_F/\tau_F = 1/(1 + \gamma k_1 \tau_F[L]) \qquad (2)$$

where $\gamma = k_3/(k_2+k_3)$ according to Eq. (1).

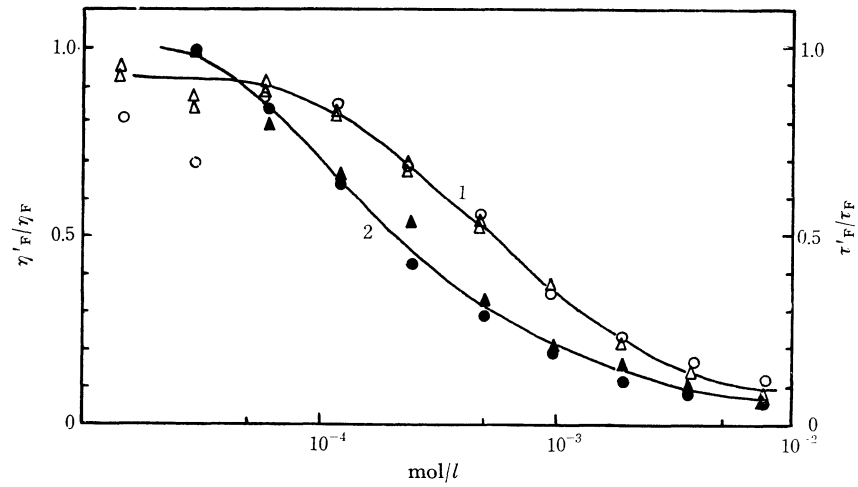

Fig. 1. η'_F/η_F or τ'_F/τ_F *vs.* [L] relations for pyrene - DMA system in acetonitrile (1) and DMF (2) at 300°K.
●, ○: η'_F/η_F ▲, △: τ'_F/τ_F [Pyrene]: 1×10^{-5} mol/l

4) N. Mataga and Y. Murata, *J. Amer. Chem. Soc.*, **91**, 3144 (1969).

The quenching rate constants γk_1 at 300°K for the pyrene-DMA system were 1.3×10^{10} l/mol·sec in acetonitrile, 5.7×10^{9} l/mol·sec in DMF and 6.9×10^{9} l/mol·sec in ethanol, respectively. Similar results have been obtained also in the case of the quenching of pyrene fluorescence by TCNB and isomeric dicyanobenzenes in polar solvents. In the case of pyrene - TCNB system in acetonitrile, the quenching curve can be reporduced accurately by Eq. (2) and the γk_1 value at 300°K has been evaluated to be 1.6×10^{10} l/mol·sec.

When isomeric dicyanobenzenes are used as quenchers, the quenching curves are not exactly reproducible by Eq. (2), but η'_F/η_F value is a little smaller than τ'_F/τ_F value at the same [L] value, although $\tau'_F/\tau_F=(1+\gamma k_1\tau_F[L])^{-1}$.

It is well-known that a more detailed consideration based on the diffusion-controlled encounter process of Eq. (3), leads to Eqs. (4) and (5).[5]

$$F^* + L \underset{k_2}{\overset{k_1}{\rightleftarrows}} F^* \cdots L \xrightarrow{k_3} \text{intermediate} \longrightarrow \quad (3)$$

$$\eta'_F/\eta_F = \delta/(1 + \gamma k_1\tau_F[L]) \quad (4)$$

$$\delta = \exp\left[-4\pi(\gamma R_0)^2\{D\tau_F(\eta'_F/\eta_F)\}^{1/2}N'[L]\right] < 1$$

$$\tau'_F/\tau_F = 1/(1 + \gamma k_1\tau_F[L]) \quad (5)$$

where, $D=D_{F^*}+D_L$, the sum of the diffusion coefficients of F* and L, N' is the Avogadro number per 1 ml and γR_0 is the effective encounter distance. When the electron transfer interaction in the encounter complex is a sufficiently short range one, Eq. (4) is reduced to the simplest case of Eq. (1) because $\delta\simeq1$.

From the results, the mechanism of Eq. (1) seems to be correct at least for the pyrene-TCNB systems.

If the mechanism of Eq. (1) is correct and the ion radicals are formed, we should be able to observe the absorption spectra of transiently produced ion radicals by means of the flash photolysis method. Actually, we have observed such spectra for pyrene - DMA system in acetonitrile as well as in ethanol (Figs. 2 and 3).

In Fig. 2, we see clearly the absorption peaks due to pyrene anion radical at 20.3×10^3, 22.0×10^3 and 26.0×10^3 cm^{-1}. The peak at *ca.* 24×10^3 cm^{-1} may be ascribed to the T-T absorption, while shoulders around this peak can neither be ascribed to the absorption of radicals nor the T-T absorption. The small shoulder at *ca.* 21.3×10^3 cm^{-1} might be assigned to the absorption band of DMA cation radical.

In the case of Fig. 3, we can observe more clearly the absorption bands of both ion radicals. The spectrum in Fig. 3c where no added DMA is present is due to the T-T absorption. In the presence of DMA((a), (b)), the absorption bands at 22.0×10^3 and 20.3×10^3 cm^{-1} due to pyrene anion radical as well as those at 22.2×10^3 and 21.3×10^3 cm^{-1} which can be ascribable to DMA cation radical have been observed. From comparison of Fig. 3b and Fig. 3a, we see that in ethanol, pyrene anion is rather unstable and decays more

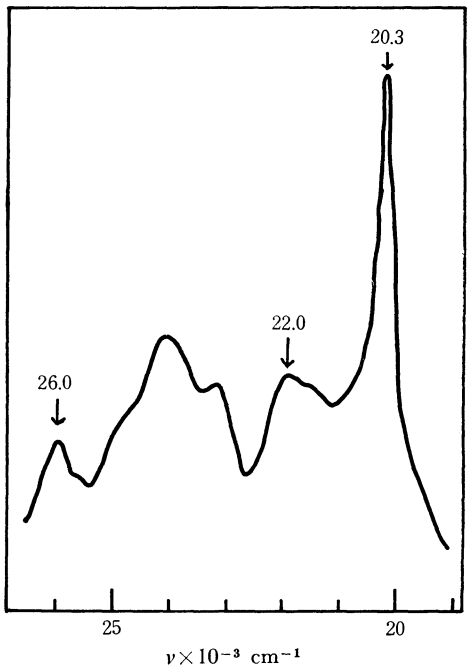

Fig. 2. Transient absorption spectra of pyrene - DMA system in acetonitrile.

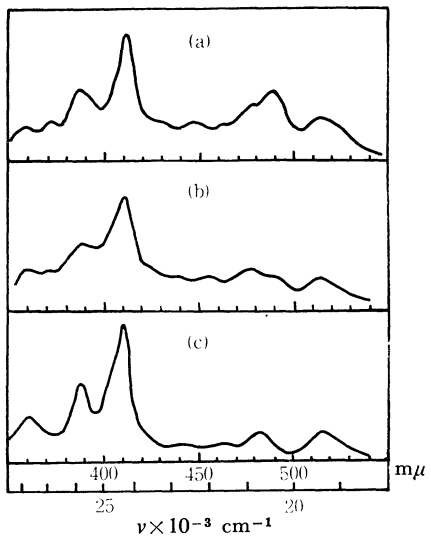

Fig. 3. Transient absorption spectra in ethanol.
(a), (b): pyrene - DMA system, the intervals between the peaks of the main flash and second one were 3 μsec(a) and 50 μsec(b)
(c): T−T absorption bands of pyrene, the interval between the two peaks was 3 μsec
[Pyrene]: 1×10^{-5} mol/l, [DMA]: 1×10^{-2} mol/l

5) A. Weller, *Z. Phys. Chem. N. F.*, **13**, 335 (1957); *ibid.*, **15**, 438 (1958); *ibid.*, **18**, 163 (1958).

rapidly compared with DMA cation. Contrary to this, the spectrum DMA cation can hardly be observed in the case of acetonitrile solution. Presumably, the ion radicals will decay partly due to the reaction with solvent molecules or unknown impurities in the solvent in addition to the bimolecular recombination reaction between anion and cation radicals (electron transfer from anion to cation). At any rate, the ion radical formation according to the mechanism of Eq. (1) has been confirmed experimentally.

The fluorescence of pyrene is quenched completely even in a non-polar solvent by the strong quencher, TCNE. The quenching curve in *n*-hexane is shown in Fig. 4. This quenching curve of pyrene - TCNE - *n*-hexane system can be well reproduced by Eq. (2); $\gamma k_1 = 2.5 \times 10^{10}$ *l*/mol·sec at 300°K. However, the formation of ion radicals cannot be observed by means of flash photolysis studies on this system. Presumably, the ion radicals are extremely unstable in this non-polar solvent. Therefore, the encounter collision may lead to the formation of charge transfer type complex which is non-fluorescent.

$$F^* + L \xrightarrow{k_1} \text{Complex} \longrightarrow \text{Product} \qquad (6)$$

Because there is a large energy difference between the state (F*+L) and the complex, the back reaction from the complex to the (F*+L) state can be neglected. The energy difference is estimated to be *ca.* 13×10^3 cm^{-1} from the CT absorption band of pyrene-TCNE CT complex and the excitation energy of pyrene.

The fluorescence of pyrene is strongly quenched by TCNE in acetonitrile solution. In contradistinction to the case of *n*-hexane solution, there is a quite large difference between the quenching curve for the fluorescence quantum yield and that for the decay time as shown in Fig. 5. Namely, $\eta'_F/\eta_F < \tau_F'/\tau_F$ for the same [L] value in general. The quenching curves in acetonitrile can be reproduced by Eqs. (4) and (5). In this polar solvent, the electron transfer from excited pyrene to TCNE may occur and ion radicals may be produced. We have confirmed by flash photolysis the transient production of TCNE anion radical in addition to the formation of pyrene cation radical with absorption band at 22.2×10^3 cm^{-1}.

We obtain from Eqs. (4) and (5),

$$\ln \delta = \ln [(\eta'_F/\eta_F)(\tau_F/\tau'_F)] = -4\pi(\gamma R_0)^2(D\tau_F)^{1/2}N'(\eta'_F/\eta_F)^{1/2}[L] \qquad (7)$$

From the plot of $\ln[(\eta'_F/\eta_F)(\tau_F/\tau'_F)]$ against $(\eta_F'/\eta_F)^{1/2}[L]$, we can obtain the value of $4\pi(\gamma R_0)^2(D\tau_F)^{1/2}N'(=v)$. As we can evaluate γk_1 from the quenching curve of (τ'_F/τ_F) and $\gamma k_1 = 4\pi\gamma R_0 DN'$, the γR_0 value can be given by

$$\gamma R_0 = [v^2/4\pi\gamma k_1 \tau_F N']^{1/3} \qquad (8)$$

Thus, it is possible to evaluate (γR_0) experimentally without knowing the value of the diffusion coefficient which, in general, does not seem to be known accurately. The γR_0 value obtained in this way was 47±8Å irrespective of the temperature at which the measurement was made. This γR_0 value is so large that one cannot regard $R_0 \geqq \gamma R_0$ as physically meaningful for the actual encounter distance in the loose complex F*···L.

It might be argued that the pyrene - TCNE CT complex is formed in the ground state, which causes the large difference between η'_F/η_F and τ'_F/τ_F values. However, this possibility can be rejected

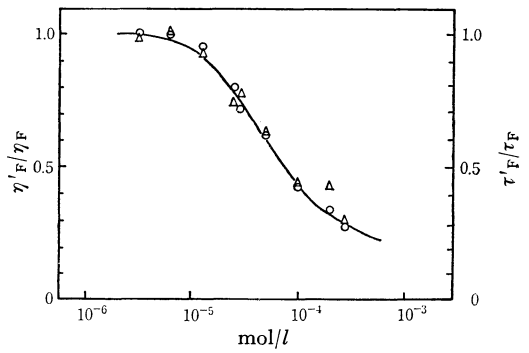

Fig. 4. Fluorescence quenching curve for pyrene - TCNE system in *n*-hexane at 300°K.
[Pyrene]: 1×10^{-5} mol/*l*, ○: η'_F/η_F, △: τ'_F/τ_F

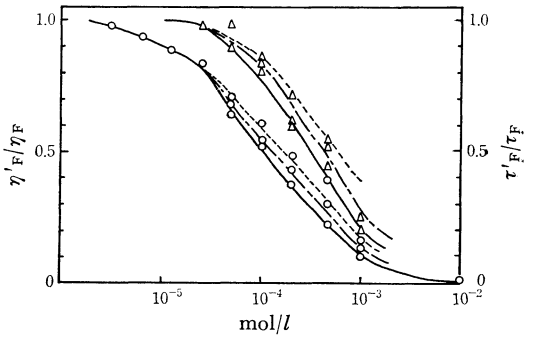

Fig. 5. Fluorescence quenching curve for pyrene - TCNE system in acetonitrile at various temperatures.
——: at 25°C, – – –: at 0°C, - - - -: at −40°C
○: η'_F/η_F, △: τ'_F/τ_F [Pyrene]: 1×10^{-5} mol/*l*

because of the fact that the absorption spectrum does not show any change in the range of TCNE concentration used here, and because of the more important fact that the extent of the quenching with respect to both of the quantum yield and the decay time is greater at higher temperatures.

One should note that Eq. (4) and, accordingly, (7) and (8) contains rather drastic approximations. One should not regard R_0 as the actual intermolecular distance in the encounter complex, in general. These approximate equations may not be

valid for this quite strong quenching action of TCNE in acetonitrile. Nevertheless, the quite strong quenching and the anomalously large R_0 value seem to indicate a long range interaction between the fluorescer and the quencher.

The diffusion equation for the encounter and electron transfer process may be written as

$$-\frac{\partial\Phi(R,t)}{\partial t} = -D\nabla^2\Phi(R,t) + \frac{1}{\tau_F}\Phi(R,t) + \sum_i W(|R-R_i|)\Phi(R,t) \qquad (9)$$

where $\Phi(R,t)$ is the distribution function for F^* and $W(|R-R_i|)$ is the electron transfer probability.

In the case of the long range electron transfer caused by the very weak interaction, $W(|R-R_i|)$ represents the electronic transition probability which depends on the intermolecular distance $|R-R_i|$ between the fluorescer and the quencher. If W is hard core type, *i.e.*,

$$\begin{aligned} W &= 0 \quad \text{at } |R-Ri| > \gamma R_0 \\ W &= 1 \quad \text{at } |R-R_i| \leqq \gamma R_0 \end{aligned} \qquad (10)$$

then the bimolecular reaction rate constant should be proportional to the diffusion coefficient D. However, if W has a long range part, the bimolecular rate constant should be proportional to D^m, where $m<1$. Such a long range effect was actually observed in the case of the singlet excitation transfer from pyrene to perylene in fluid solution,[6] where W has been proved to be proportional to inverse sixth power of $|R-R_i|$.[7] Namely, it has been confirmed that the bimolecular rate constant for the quenching of pyrene fluorescence caused by the excitation transfer is proportional to D when the D value is relatively large, while it is proportional to $D^{3/4}$ at relatively small values of D in accordance with the theoretical consideration.[8]

From the viewpoint of the above consideration, we have examined the dependence of γk_1 value (which can be determined accurately by the measurement of the decay times) on the diffusion coefficient for the pyrene - TCNE - acetonitrile system.

The temperature dependences of $1/\tau_F$ and $1/\tau'_F$ values are shown in Fig. 6. These curves were obtained by repeating the measurement of the decay time many times at each temperature and averaging them. The accuracy of the measurement was not so good for curve (4) compared to the others, because of a little smaller number of measure-

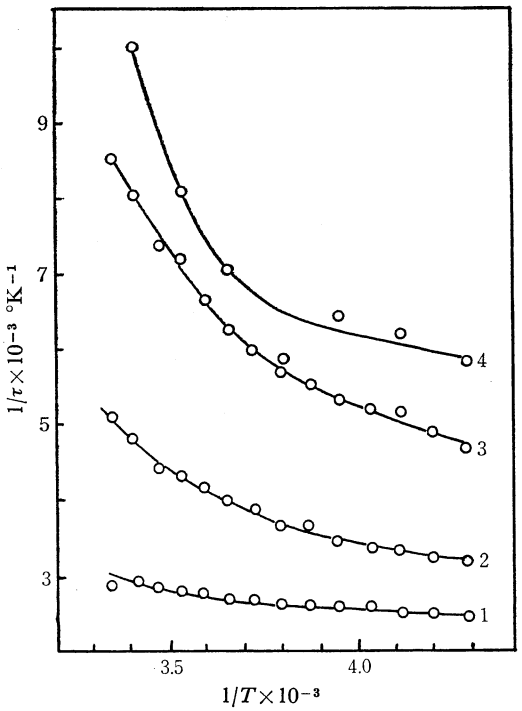

Fig. 6. $1/\tau_F$ or $1/\tau'_F$ *vs.* $1/T$ relations for pyrene - TCNE system in acetonitrile.
[TCNE]: (1) 0, (2) 2×10^{-4}, (3) 4×10^{-4}, (4) 9×10^{-4} mol/*l*, [Pyrene]: 1×10^{-5} mol/*l*

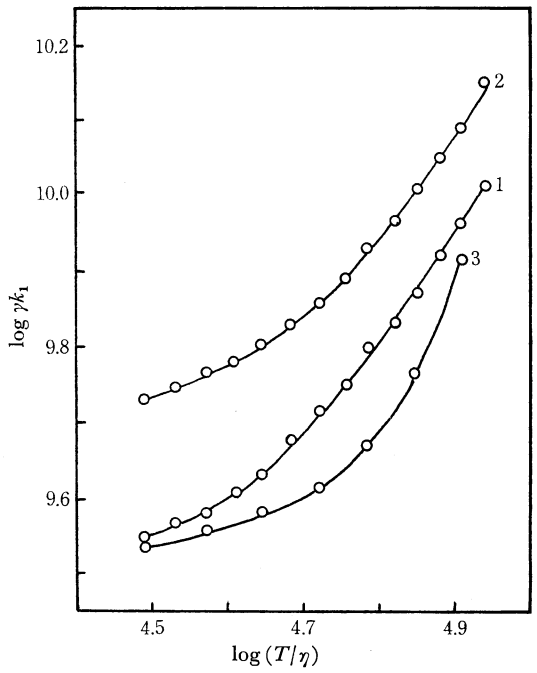

Fig. 7. log γk_1 *vs.* log (T/η) relations for pyrene - TCNE system in acetonitrile.
[TCNE]: (1) 2×10^{-4}, (2) 4×10^{-4}, (3) 9×10^{-4} mol/*l*, [Pyrene]: 1×10^{-5} mol/*l*

6) M. Tomura, E. Ishiguro and N. Mataga, *J. Phys. Soc. Japan*, **22**, 1117 (1967); *ibid.*, **25**, 1439 (1968).

7) N. Mataga, H. Obashi and T. Okada, *Chem. Phys. Lett.*, **1**, 133 (1967); *J. Phys. Chem.*, **73**, 370 (1969).

8) M. Yokota and O. Tanimoto, *J. Phys. Japan*, **22**, 779 (1967).

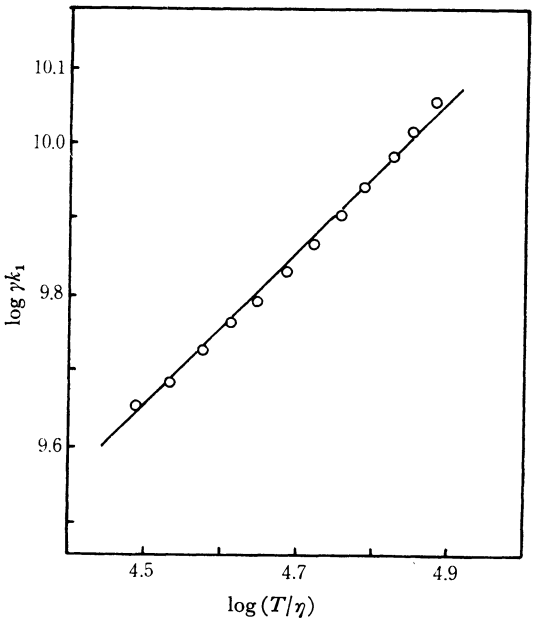

Fig. 8. log γk_1 *vs.* log (T/η) relation for pyrene - DMA system in acetonitrile.
[Pyrene]: 1×10^{-5} mol/*l*, [DMA]: 4×10^{-4} mol/*l*

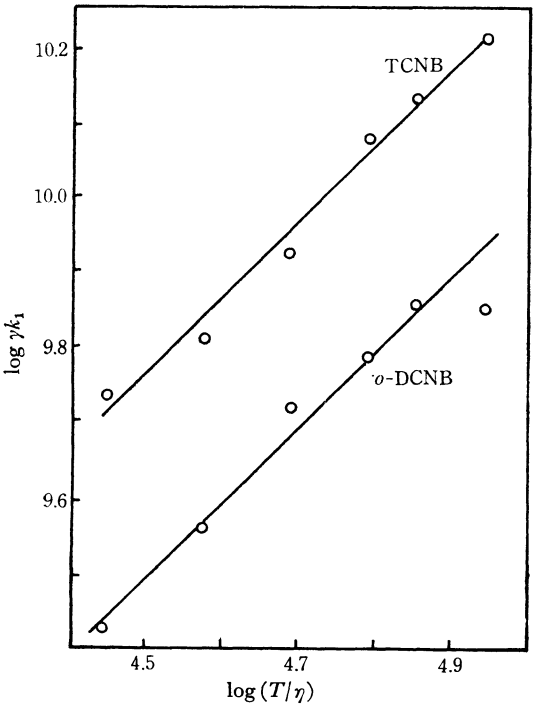

Fig. 9. log γk_1 *vs.* log (T/η) relations for pyrene - TCNB and pyrene - *o*-DCNB systems in acetonitrile.

ments. From these values of decay times, the γk_1 values have been obtained by means of the equation $\gamma k_1=(\tau_F/\tau_F'-1)/\tau_F[L]$.

In Fig. 7, log γk_1 values are plotted against log (T/η), where T is the absolute temperature and η is the viscosity of the solution. Although the absolute value of γk_1 for each [L] value is not very accurate, the shapes of the curves in Figs. 6 and 7 are certainly reliable. Of course, the correction for the change of the concentration of the quencher due to the change of the temperature of the solution has been taken into concideration. As (T/η) is proportional to the diffusion coefficient, this plot will provide the desired information as described above.

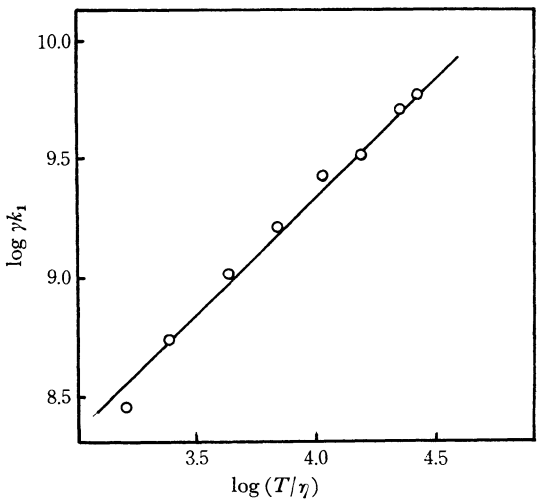

Fig. 10. Log γk_1 *vs.* log (T/η) relation for pyrene - *p*-DCNB system in ethanol.
[*p*-DCNB]: 1×10^{-3} mol/*l*, [Pyrene]: 1×10^{-5} mol/*l*

We see clearly from Fig. 7, that $m\simeq1$ in the range of relatively large (T/η) values, while $m<1$ at relatively small (T/η) values. Moreover, the long range effect appears to be more predominant in the case of higher concentrations of TCNE. Thus, the long range electron transfer process due to the very weak interaction seems to play an important role and the hard sphere model provides only a poor approximation for the pyrene - TCNE system in acetonitrile.

As the fluorescence quenching reaction of pyrene-DMA system in acetonitrile can be reproduced satisfactorily by Eq. (2) the long range effect may not be important in this system. Thus, one may expect a straight line with $m=1$ when log γk_1 is plotted against log (T/η). The relation is actually satisfied (Fig. 8).

Since quite an analogous result to the case of pyrene - DMA system has been observed for the quenching curve of pyrene-TCNB system in acetonitrile, we can expect that $m\simeq1$ also for this system. When *p*-DCNB and *o*-DCNB were used as quenchers for pyrene fluorescence in acetonitrile solution, there is a little tendency that $\eta'_F/\eta_F\lesssim\tau_F'/\tau_F$. By means of Eqs. (7) and (8), the γR_0 values have been evaluated to be 29Å for *p*-DCNB and 24Å

for *o*-DCNB in acetonitrile. These γR_0 values are much smaller than in the case of the fluorescence quenching due to TCNE. Therefore, it is possible that a similar result to the case of pyrene-TCNB system (*i.e.* $m \simeq 1$) can be obtained also for the pyrene - *o*-DCNB system, because the difference between the value of η'_F/η_F and that of τ'_F/τ_F is rather small.

As indicated in Fig. 9, log γk_1 is linear with log (T/η) and $m \simeq 1$ for both systems. In contrast to this, although log γk_1 is approximately linear with log (T/η), m is a little smaller than unity in the case of pyrene - *p*-DCNB system in acetonitrile. We have further examined pyrene - *p*-DCNB system in ethanol and also, in pyridine solution. Although η'_F/η_F is a little smaller than τ'_F/τ_F in ethanol solution, γk_1 is proportional to (T/η) and $m \simeq 1$ as shown in Fig. 10. In the case of pyridine solution, the quenching curve and the change of the fluorescence spectrum are shown in Figs. 11 and 12, respectively. The quenching curve can be well reproduced by the simple Stern-Volmer equation (2). However, as shown in Fig. 12, one can observe the fluorescence of pyrene - *p*-DCNB exciplex. Since the yield of this exciplex fluorescence is quite small, it is probable that the ion-pair formation process (k_3) as indicated in Eq. (1), is competing with the fluorescence transition, the probability of which may be rather small because of the very polar structure of the exciplex. In a more polar solvent such as ethanol, process k_3 is certainly much more dominant than the exciplex fluorescence transitions so that the exciplex fluorescence cannot be observed in ethanol solution.

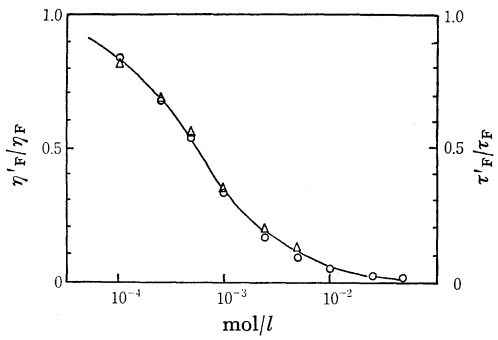

Fig. 11. η'_F/η_F or τ'_F/τ_F *vs.* [L] relation for pyrene - *p*-DCNB system in pyridine at 25°C.
○: η'_F/η_F, △: τ'_F/τ_F

We can summarize the results as follows. In non-polar and less polar solvents, the exciplex formation occurs between the fluorescer and the quencher molecules. The exciplex is either fluorescent or non-fluorescent. Furthermore, in a slightly polar solvent, there arises a solvated ion-pair via the exciplex. In the more polar solvents, there occurs an electron transfer from the fluorescer to the quencher and *vice versa* due to the short

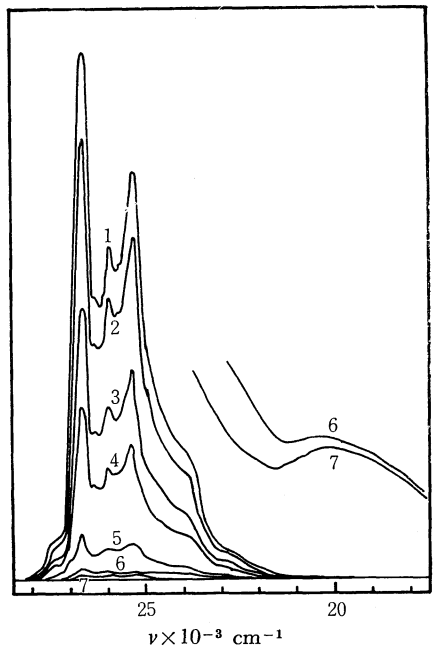

Fig. 12. Fluorescence spectra of pyrene - *p*-DCNB in pyridine at 25°C.
[*p*-DCNB]: (1) 0, (2) 1×10^{-4}, (3) 5×10^{-4}, (4) 1×10^{-3}, (5) 5×10^{-3}, (6) 2.5×10^{-2}, (7) 5×10 mol/l
[Pyrene]: 1×10^{-5} mol/l

range interaction or the long range very weak interaction depending on the strength of the quencher. The long range electron transfer process due to the very weak interaction may be a non-adiabatic quantum mechanical transition as will be described below.

Let us denote the energies of the various states in Eq. (1) as follows: $U_1=U(F^*+L)$, $U_2=U$ (exciplex), $U_3=U(F_S^{\pm}\cdots L_S^{\mp})$ and $U_4=U(F_S^{\pm}+L_S^{\mp})$ When $U_2^\circ > U_3^\circ$ or U_4°, the solvated complex will immediately shift to the solvated ion-pair or dissociate into the solvated ion radicals, where U_i°'s represent the values for the equilibrium state with respect to the solute-solvent interactions. If the interaction between the fluorescer and the quencher is not very weak, the reaction will proceed on the adiabatic potential energy surface and the probability W may be of a hard core type.

When the interaction between the partners in the exciplex is weak, its wavefunction may be written as

$$\Psi \sim c_1(s)\Phi_i^\circ(F^*\cdots L) + c_2(s)\Phi_f^\circ(F^+\cdots L^-)$$
$$\text{or} \qquad (11)$$
$$\Psi \sim c_1(s)\Phi_i^\circ(F^*\cdots L) + c_2(s)\Phi_f^\circ(F^-\cdots L^+)$$

where s symbolizes the nuclear configurations including the surrounding solvent molecules. When the electronic interaction between F* and L in the loose encounter complex F*···L is very weak

in a sufficiently polar solvent, the isoenergetic electronic transition will occur from the state Φ_i° to Φ_f°. The electron transfer by this process may be given schematically by configuration coordinate diagrams as shown in Fig. 13. In this figure, the long range electron transfer is represented by the quantum mechanical tunnelling through the potential barrier as indicated by the horizontal wavy line. In the case of curve (a) for U_3, the barrier may be too high for the tunnelling to occur while it may be possible in the case of curve (b).

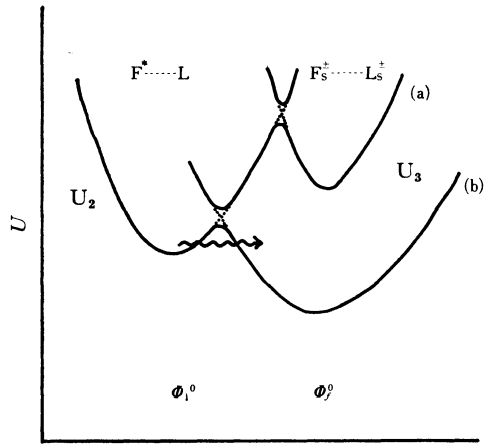

Fig. 13. Schematic diagrams of the electron transfer process by very weak interaction.

The energy of the curve U_3 depends upon the magnitudes of ionization potential of the donor and the electron affinity of the acceptor on the one hand and upon the solvation energies of the ion radicals on the other hand. Among the cyano compounds used in the present work, the electron affinity of TCNE is the largest. Moreover, the solvation energy of its anion in polar solvent may be the largest because its molecular radius is the smallest among others. Therefore, U_3 may be the lowest in the case of pyrene - TCNE - acetonitrile system.

The tunnelling efficiency depends also upon the magnitude of the matrix element of the perturbation Hamiltonian between Φ_i° and Φ_f°. As the spatial dimension of TCNE is the smallest among the quenchers employed, the overlap between the electron donating orbital of excited pyrene and the accepting orbital of TCNE may be large compared to those of the other systems, which results in a relatively large value of the perturbation matrix element.

We have discussed the long range electron transfer in analogy to the long range singlet-singlet excitation transfer. Let us examine the matrix elements responsible for the excitation transfer as well as the electron transfer transition. We assume both F and L are closed shell molecules and denote their MO's as ψ_m^F's and ψ_m^L's respectively, where the m-th MO's are the highest occupied ones in the ground state. The Hamiltonian $\mathscr{H}$ can be separated into the core part $\mathscr{H}_c=\sum f_c(i)$ and the electron interaction part $G=\sum g(ij)$. Then, the matrix elements for the following excitation transfer processes

$$F^*(^1L_a) + L \rightarrow F + L^*(^1L_a)$$
$$F^*(^1L_b) + L \rightarrow F + L^*(^1L_a)$$

can be written as

$$\langle\Phi_i^\circ(^1L_a)|\mathscr{H}|\Phi_f^\circ(^1L_a)\rangle = 2(\langle\psi_m^L\psi_{m+1}^F|g|\psi_{m+1}^L\psi_m^F\rangle - \langle\psi_m^L\psi_{m+1}^F|g|\psi_m^F\psi_{m+1}^L\rangle) \quad (12a)$$

$$\langle\Phi_i^\circ(^1L_b)|\mathscr{H}|\Phi_f^\circ(^1L_a)\rangle = \sqrt{2}(\langle\psi_m^L\psi_{m+2}^F|g|\psi_{m+1}^L\psi_m^F\rangle - \langle\psi_m^L\psi_{m+2}^F|g|\psi_m^F\psi_{m+1}^L\rangle - \langle\psi_m^L\psi_{m+1}^F|g|\psi_{m+1}^L\psi_{m-1}^F\rangle + \langle\psi_m^L\psi_{m+1}^F|g|\psi_{m-1}^F\psi_{m+1}^L\rangle) \quad (12b)$$

In contrast to this, the matrix elements for the electron transfer transitions

$$F^*(^1L_a)\cdots L \rightarrow F^+\cdots L^-$$
$$F^*(^1L_b)\cdots L \rightarrow F^+\cdots L^-$$

are given by[3]

$$\langle\Phi_i^\circ(^1L_a)|\mathscr{H}|\Phi_f^\circ(F^+\cdots L^-)\rangle = \langle\psi_{m+1}^F|f_c|\psi_{m+1}^L\rangle + \sum_{\lambda_k\neq\psi_{m+1}^F}\{\langle\psi_{m+1}^F\lambda_k|g|\psi_{m+1}^L\lambda_k\rangle - \langle\psi_{m+1}^F\lambda_k|g|\lambda_k\psi_{m+1}^L\rangle\} + \langle\psi_m^F\psi_{m+1}^F|g|\psi_{m+1}^L\psi_m^F\rangle \quad (13a)$$

$$\langle\Phi_i^\circ(^1L_a)|\mathscr{H}|\Phi_f^\circ(F^+\cdots L^-)\rangle = \frac{1}{\sqrt{2}}[\langle\psi_{m+1}^F|f_c|\psi_{m+1}^L\rangle + \sum_{\lambda_k\neq\psi_{m+2}^F}\{\langle\psi_{m+2}^F\lambda_k|g|\psi_{m+1}^L\lambda_k\rangle - \langle\psi_{m+2}^F\lambda_k|g|\lambda_k\psi_{m+1}^L\rangle\} + \langle\psi_{m+1}^F\psi_m^F|g|\psi_{m+1}^L\psi_{m-1}^F\rangle + \langle\psi_m^F\psi_{m+2}^F|g|\psi_{m+1}^L\psi_m^F\rangle - 2\langle\psi_{m+1}^F\psi_m^F|g|\psi_{m-1}^F\psi_{m+1}^L\rangle] \quad (13b)$$

For the excitation transfer, only the electron interaction integral plays an important role while both the core part and the electron interaction part may be important for the electron transfer. It is well-known that the Coulomb integral in $\langle\Phi_i^\circ|\mathscr{H}|\Phi_f^\circ\rangle$ plays the dominant role for the excitation transfer. Since the matrix elements in the r.h.s. of Eqs. (13a,b) are roughly proportional to the intermolecular overlap of MO's, the transition matrix elements for the electron transfer will be smaller than the Coulomb integrals (which do not depend on the intermolecular overlap) in Eq. (12), at a sufficiently large intermolecular distance. However, the matrix elements in Eq. (13) have a much longer range interaction than the corresponding matrix element for the triplet-triplet excitation transfer, where the electron exchange integral which is roughly proportional to the square of the intermolecular overlap plays the dominant role.

Although only the electronic part of the interaction is shown in Eqs. (12) and (13), Φ^0's are

also function of the nuclear coordinates of solute as well as the surrounding solvent molecules. As U's are adiabatic potential energies, the tunnelling may be caused essentially by the vibronic interactions between transferring electron and the nuclear motions. Presumably, the interaction process between the polarization motion (mainly orientational) of the solvent molecules and the transferring electron is the dominant mechanism for tunnelling. This sort of interaction may be large in a polar solvent such as acetonitrile, which is in accord with the observed results.

The intermolecular electron transfer by very weak interaction in the excited state, as demonstrated here, will be found out for other systems. Studies along this line are in progress.